THE JOURNAL OF BIOLOGICAL CHEMISTRY VOL. 288, NO. 10, pp. 7420–7429, March 8, 2013

Kir2.4 Surface Expression and Basal Current Are Affected by Heterotrimeric G-Proteins*

Received for publication, August 23, 2012, and in revised form, January 11, 2013 Published, JBC Papers in Press, January 21, 2013, DOI 10.1074/jbc.M112.412791

Pyroja Sulaiman[‡], Ying Xu[§], Marie E. Fina[‡], Shanti R. Tummala[‡], Hariharasubramanian Ramakrishnan[‡], Anuradha Dhingra[‡], and Noga Vardi[‡1]

From the [‡]Department of Neuroscience, Perelman School of Medicine, University of Pennsylvania, Philadelphia, Pennsylvania 19104 and [§]Joint Laboratory for Brain Function and Health, Jinan University and the University of Hong Kong, Jinan University, 510632 Guangzhou, China

Background: Basal activity of the inward rectifying potassium channel Kir2.4 is important for a variety of neuronal functions.
Results: Pertussis toxin-sensitive Gα subunits reduce basal current and surface expression of Kir2.4, whereas G$\beta\gamma$ increases them.
Conclusion: Heterotrimeric G-proteins regulate the surface expression of potassium channels.
Significance: This study extends the role of G-protein subunits in modulating neuronal physiology by regulating the expression of channel proteins.

Kir2.4, a strongly rectifying potassium channel that is localized to neurons and is especially abundant in retina, was fished with yeast two-hybrid screen using a constitutively active $G\alpha_{o1}$. Here, we wished to determine whether and how $G\alpha_o$ affects this channel. Using transfected HEK 293 cells and retinal tissue, we showed that Kir2.4 interacts with $G\alpha_o$, and this interaction is stronger with the GDP-bound form of $G\alpha_o$. Using two-electrode voltage clamp, we recorded from oocytes that were injected with Kir2.4 mRNA and a combination of G-protein subunit mRNAs. We found that the wild type and the inactive mutant of $G\alpha_o$ reduce the Kir2.4 basal current, whereas the active mutant has little effect. Other pertussis-sensitive Gα subunits also reduce this current, whereas $G\alpha_s$ increases it. G$\beta\gamma$ increases the current, whereas *m*-phosducin, which binds G$\beta\gamma$ without affecting the state of Gα, reduces it. We then tested the effect of G-protein subunits on the surface expression of the channel fused to cerulean by imaging the plasma membranes of the oocytes. We found that the surface expression is affected, with effects paralleling those seen with the basal current. This suggests that the observed effects on the current are mainly indirect and are due to surface expression. Similar results were obtained in transfected HEK cells. Moreover, we show that in retinal ON bipolar cells lacking Gβ3, localization of Kir2.4 in the dendritic tips is reduced. We conclude that G$\beta\gamma$ targets Kir2.4 to the plasma membrane, and $G\alpha_o$ slows this down by binding G$\beta\gamma$.

Heterotrimeric G-proteins play diverse roles in biological systems. Their major role lies in coupling metabotropic receptors to a variety of effectors. In this role, G-protein subunits stimulate or inhibit a diverse number of effectors, including ion channels (reviewed by Ref. 1). In an effort to find retinal interactors for the constitutively active subunit $G\alpha_o$, the subunit that is required for the retinal ON bipolar light response, we previously fished many known G-protein modulators and the inwardly rectifying potassium channel, Kir2.4 (2–5). The Kir channel family is divided into four subfamilies (Kir1–4) with the Kir3 subfamily being directly gated by G$\beta\gamma$ (reviewed by Refs. 6–12). Gα also binds this subfamily and plays an important role in reducing the basal activity of this channel and priming it so that it can be gated more efficiently by G$\beta\gamma$ (13–16). The other Kir subfamilies are not known to be directly modulated by G-proteins, although they are modulated by phosphorylation mediated by G-protein-coupled receptors (17–19).

The Kir2 channels inwardly rectify more strongly than the other Kir subfamilies (6, 7, 20). Their general function is adjusting neuronal excitability, contributing to resting potential and metabolic processes in neural and non-neural tissues. Kir2.4 was initially cloned from the brain; it was found in several regions, most strongly in motorneurons of cranial nuclei, and the human form was found to be particularly abundant in retina, where it is expressed in most cell types (21–23). Kir2.4 subunits can form homotetrameric channels as well as heterotetramers with other members of Kir2 family such as Kir2.1, and these different stoichiometries have been suggested to provide physiological heterogeneities (24). Having fished the Kir2.4 by $G\alpha_o$, we wished to know whether these proteins functionally interact. Specifically, we wanted to determine whether the activity of Kir2.4, similar to Kir3 activity, is modulated by G-proteins. We thus recorded the activity of this channel in *Xenopus* oocytes with and without the co-expression of different G-protein subunits. We found that $G\alpha_{i/o}$ severely reduces Kir2.4 surface expression and its basal current, whereas G$\beta\gamma$ increases them. Our data expand the repertoire of G-protein functions beyond their essential and dominant effect of coupling receptors to downstream signaling processes.

* This work was supported by National Institutes of Health Grants EY11105 (to N. V.) and NEI P30 EY01583 (Vision Research Core of the University of Pennsylvania).
[1] To whom correspondence should be addressed: Dept. of Neuroscience, Perelman School of Medicine, University of Pennsylvania, Philadelphia, PA 19104. Tel.: 215-898-4520; Fax: 215-898-6228; E-mail: noga@mail.med.upenn.edu.

MATERIALS AND METHODS

cDNA Constructs and mRNA—Kir2.4 was amplified by RT-PCR from mouse retinal RNA prepared using a Nucleospin RNA II kit (Clontech). Reverse transcription was performed on 1 μg of total RNA with oligo-dT primers using Moloney murine leukemia virus reverse transcriptase (BD Biosciences). The primers used for PCR were as follows: 5′-agg aca gat cta gag ggg gtc t-3′ (forward) and 5′-cat cag agg ctg gaa gga ag-3′ (reverse). PCRs used 35 cycles (94 °C for 1 min, 58 °C for 30 s, and 72 °C for 2 min) and were performed on a programmable thermocycler (PerkinElmer Life Sciences). The PCR product was then subcloned into pcDNA3.1 using pcDNA3.1/V5-His TOPO TA expression vector (Invitrogen) to yield Kir2.4-pcDNA3.1.

Kir2.4-cerulean (Kir-cer, fused at the Kir2.4 N terminus) construct was prepared by amplifying the cerulean from *m*-Cerulean-C1 (a kind gift from Dr. Matthew Dalva, Jefferson University, Philadelphia, PA) using the following primers: 5′-agc agc aag ctt atg gtg agc aag ggc gag gag ctg-3′ (forward) and 5′-agc agc cca cga tgg gga ctt gta cag ctc gtc cat gcc-3′ (reverse). PCR product and Kir.2.4-pcDNA3.1 vector were digested with BSrG1. The following clones (in pGEMHE or its derivative pGEMHJ; high-expression oocyte vectors containing 5′- and 3′-untranslated sequences of *Xenopus* β-globin) were gifts from Dr. Nathan Dascal (Tel-Aviv University, Israel): $G\alpha_{o1}$, $G\alpha_{i1}$, $G\alpha_{i3}$, $G\alpha_{s}$, $G\beta1$, $G\gamma2$, and *m*-phosducin. The $G\alpha_{o2}$ clone (in pAGA-2) was a gift from Dr. Lutz Birnbaumer (NIH, Research Triangle Park, NC), and it was subcloned into pGEMHJ. $G\alpha_{o1}$ (in pDP) was provided by Dr. David Manning (University of Pennsylvania, PA). $G\alpha13$ and $G\alpha_{q}$ (in pCDNA) were obtained from UMR cDNA Resource Center (Rolla, MO). $G\beta1$ and $G\gamma2$ cDNA (in pCDNA3.1) were provided by Dr. Kirill Martemyanov (The Scripps Research Institute). For oocyte injections, DNA plasmids containing the various clones were linearized with the appropriate restriction enzymes using a standard protocol, and mRNAs were synthesized *in vitro* using mMessage mMachine Kit (Ambion, USA). The injected volume of RNA mixture was 41.4 nanoliters.

Cell Culture, Transfection, and Co-immunoprecipitation—Human embryonic kidney (HEK) 293 cells were cultured in minimal essential medium supplemented with Penstrep (Invitrogen) and 10% heat-inactivated fetal bovine serum at 37 °C in a 5% CO_2 incubator. Cells were transiently transfected with Kir2.4 (in pcDNA3.1) and $G\alpha_{o1}$ (in pDP) using FuGENE 6 transfection reagent (Invitrogen). Cells were harvested 24 h later. HEK 293T-transfected cells or mouse retinal homogenates were collected in lysis buffer (50 mM Tris, pH 7.4, 150 mM NaCl, 1 mM EDTA, 1% Triton X-100, 5 mM $MgCl_2$, 100 μM GDP, 30 mM PMSF) with or without AlF_4^- (30 μM $AlCl_3$ and 10 mM NaF). The cells were homogenized at low speed and centrifuged at 8,000 × *g* in an Eppendorf centrifuge for 5 min. The supernatant was precleared by adding 20 μl of protein G agarose beads (Invitrogen), centrifuging, and collecting the supernatant. The precleared supernatant was incubated with mouse anti-$G\alpha_{o}$ and protein G agarose beads on a rotator at 4 °C for ~12 h. The beads with protein complexes were then pulled down by centrifuging (10,000 × *g*), washed thoroughly in lysis buffer, resuspended in Laemmli buffer, boiled, and spin filtered. The proteins were run on 10% SDS-PAGE gel and transferred to a nitrocellulose membrane using semi-wet transfer apparatus (Bio-Rad). Blots were then incubated sequentially in the following: 10% nonfat dry milk in PBS containing 0.1% Tween 20 (PBST) at 4 °C for 1 h, primary antibodies (against $G\alpha_{o1}$ or Kir2.4, both raised in rabbit) in PBST at 4 °C overnight, PBST, and secondary antibodies linked to HRP. Protein bands were detected by SuperSignal West Femto Maximum Sensitivity Substrate (Pierce Biotechnology).

Antibodies—We used mouse anti-$G\alpha_{o}$ (mAb 3073) from Millipore (Billerica, MA); rabbit anti $G\alpha_{o}$, a gift from Dr. Manning (University of Pennsylvania); rabbit anti-Kir2.4, a gift from Dr. Rudiger Veh (Institut fur Integrative Neuroanatomie, Berlin, Germany; (see Ref. 5); guinea pig anti-mGluR6 (Neuromics, Inc., Northfield, MN); rabbit anti-GFP from Millipore (Temecula, CA); rabbit anti-$G\beta1$(SC-379, Santa Cruz Biotechnology, Inc., Santa Cruz, CA), anti-rabbit Fab fragments linked to HRP from Protos (Burlingame, CA), and anti-mouse F(ab′)2 linked to Cy3 (Jackson ImmunoResearch Laboratories, West Grove, PA).

Electrophysiology—*Xenopus* oocytes were isolated and prepared as described previously (25) or were obtained already prepared from the laboratory of Dr. Zhe Lu (University of Pennsylvania). All experiments were carried out in accordance with the University of Pennsylvania Institutional Animal Care and Use Committee. Oocytes were injected with mRNA and incubated for 2–3 days in physiological ND96 solution (96 mM NaCl; 2 mM KCl; 1 mM $CaCl_2$; 1 mM $MgCl_2$; and 5 mM Hepes/NaOH; pH 7.5, and adjusted using NaOH) supplemented with streptomycin (100 μg ml^{-1}) and penicillin (62.75 μg ml^{-1}). Experiments were performed at room temperature (20–22 °C). Kir2.4 currents were measured with a two-electrode voltage clamp using Oocyte clamp OC-725 (Warner Instruments). Electrodes were filled with 3 M KCl, and their resistances were ~2 megohms. High K^+ 24 solution was as follows: 24 mM KCl; 74 mM NaCl; 1 mM $CaCl_2$; 1 mM $MgCl_2$; 5 mM Hepes; pH 7.5, adjusted with KOH. High K^+ 96 solution consisted of the following: 96 mM KCl; 2 mM NaCl; 1 mM $CaCl_2$; 1 mM $MgCl_2$; 5 mM Hepes; pH 7.5, adjusted with KOH. Cells were clamped to −80 mV, and the holding current was measured under different conditions. For conductance measurements, a voltage ramp was applied from −150 to +30 mV for 2 s. Current signals were filtered at 1 kHz; data acquisition and analysis were done using pCLAMP software (Molecular Devices). In each experiment (*i.e.* batch of oocytes), the average current of uninjected oocytes was subtracted from the current recorded for each injected oocyte, and this was normalized to the average current of the group injected only with Kir2.4 mRNAs. These normalized currents were then averaged across experiments and subjected to a Student's *t* test.

Quantifying Kir2.4-cer Surface Expression—Oocytes injected with Kir2.4-cerulean were imaged with a confocal microscope (Olympus FV-1000) under water immersion 10× objective (numerical aperture of 1). The focal plane was adjusted to obtain the brightest image (usually at the largest perimeter). To capture a representative average of the expression throughout the oocytes, we took care to place the oocytes so that the imaged equator contained both the animal and the vegetal hemispheres

of the oocytes. An annulus was drawn around the fluorescent region at the oocyte perimeter, and the average intensity was calculated (with Fluoview 1000; dynamic range, 12 bit). A circular region at the middle of the oocyte was used to calculate the mean background fluorescence, and this value was subtracted from the average perimeter value. In each experiment, uninjected oocytes were also measured, and their average fluorescent value was also subtracted from the fluorescent value of each injected oocyte. All imaging parameters (*e.g.* laser power, offset, gain, etc.) remained the same for all oocytes.

We initially assessed several methods for quantification taking care to include the full oocyte in the field of view. In one method, we took the average value of the whole field without drawing regions of interest. In another method, we imaged the top surface of the oocyte in case this revealed a larger area and a better representation of the expression. And yet, in two other methods, we focused until we obtained the largest circle or the brightest circle. We then plotted fluorescent values *versus* basal current and computed the correlation between these parameters; the best correlation was obtained when the brightest large circle was in focus, hence the choice of this method as described in the previous paragraph.

Immunostaining—Wild type (WT) C57BL/6J mice were purchased from Charles River Laboratories; the *Gnb3*-null mouse was described in Ref. 26, and the *Gnao1*-null mouse was described in Ref. 3. Mice were treated in compliance with federal regulations and University of Pennsylvania policy. Mice were deeply anesthetized by intraperitoneal injection of a mixture of 100 μg/gm ketamine and 10 μg/gm xylazine; the eyes were enucleated, and the mouse was killed by anesthetic overdose. Both male and female mouse tissues were used.

The eyeball was fixed in 4% paraformaldehyde for 10 min and cryoprotected and embedded in a mixture of two parts 20% sucrose in phosphate buffer and one part tissue freezing medium. The eye was cryosectioned radially at 10–15-μm thickness. Retinal cryosections or fixed HEK cells were soaked in diluent containing 1.5% normal goat serum, 5% sucrose, and 0.5% Triton X-100 in phosphate buffer. Samples were incubated in primary antibodies at 4 °C for 3 days (retina) or overnight (HEK cells); washed; incubated for 3 h in secondary antibodies conjugated to a fluorescent marker; rinsed; and mounted in Vectashield (Vector Laboratories, Burlingame, CA). Retinal slices or transfected HEK cells were photographed under a confocal microscope (Olympus FL1000) with a ×60 lens with zoom 2. For retinal immunostaining comparison, a set of age-matched wild type and null retinas were simultaneously processed and imaged under the same settings.

Evaluation of Kir2.4 Distribution in Transfected HEK cells—To determine the number of cells with membrane localization of Kir2.4, we visually inspected transfected cells throughout their depth and simply counted those that showed an outline and those that did not (*i.e.* showed only an accumulation of stain in the cytoplasm). To get a representative intensity profiles, we drew a line along the diameter of each cell expressing Kir2.4 and plotted the intensities along this line. The starting point of each line was slightly outside the membrane (as detected by staining for $G\alpha_{o1}$ or $G\beta$) at a region where no large intracellular Kir2.4 expression was present (so that Kir2.4-cer

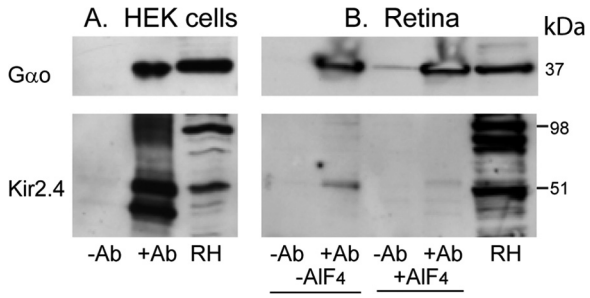

FIGURE 1. **Kir2.4 co-immunoprecipitates with $G\alpha_o$ in HEK cells and in retina.** $G\alpha_o$ was precipitated with a monoclonal antibody in HEK cells (*A*) and retinal tissue (*B*), and Kir2.4 was probed with rabbit anti-Kir2.4. *Top panels* show the $G\alpha_o$ bands; *lower panels* show the pulled Kir2.4 bands. Anti-Kir2.4 typically reveals a monomer and a dimer. In HEK cells, both were often pulled; in retina, only the monomer was precipitated. *RH*, retinal homogenate (20 μg protein was loaded). Some retinal samples were pretreated with AlF_4^- to stabilize $G\alpha_o$ in the active transition state; Kir2.4 co-immunoprecipitation is better in the absence of AlF_4^-.

expression at this point was either sharp or absent; see examples in Fig. 7, *J* and *K*). The line then progressed through the cell to the other end passing through an intracellular region with high level of expressed Kir2.4. The intensity profile of the line provides a semiquantitative visual display of the relative distribution of Kir2.4 near or at the membrane (on the *left* of the graph) to that in the cytoplasm (broad staining on the *right*). Using a Matlab program, multiple lines from multiple cells were aligned according to the membrane location, as determined by the peak of the staining for $G\alpha_o$ or $G\beta\gamma$.

RESULTS

Kir2.4 Interacts with $G\alpha_o$—Kir2.4 was identified as an interactor for $G\alpha_o$ in the yeast two-hybrid system, so it was important to determine whether these two proteins also interact in the mammalian system. We addressed this question by performing co-immunoprecipitation on HEK cells transfected with mouse Kir2.4 and $G\alpha_o$. We chose to use a mouse sequence because most of our physiologically relevant work is performed on mouse retina. Amplifying and sequencing the coding region of this message showed the sequence to be identical to that for mouse embryonic Kir2.4 transcript, a provisional RefSeq record in the GenBank (accession no. NM_145963). The coding sequence was 96 and 88% identical to the rat and human Kir2.4 sequence, respectively.

Immunoprecipitating $G\alpha_o$ with a monoclonal antibody pulled down Kir2.4, whereas omitting anti-$G\alpha_o$ did not (Fig. 1*A*, five experiments). When retinal samples were used for co-immunoprecipitation, only three of five experiments produced Kir2.4 bands. Nevertheless, in these three experiments, more Kir2.4 was pulled down when we omitted $ALF4^-$, an activator of $G\alpha$ that promotes a conformation mimicking the transition stage for GTP hydrolysis (Fig. 1*B*). The interaction between these two proteins raises the possibility that $G\alpha_o$, most likely in its GDP-bound form, modulates Kir2.4 channel activity.

Properties of Mouse Kir2.4 Current—Because our Kir2.4 sequence was cloned from mouse retina, we first tested its characteristics. Messenger RNA of Kir2.4 (1 ng) was injected into *Xenopus* oocytes and the basal current of the channel was measured using two-electrode voltage clamp recordings. In all experiments, oocytes were clamped to −80 mV in ND96 solu-

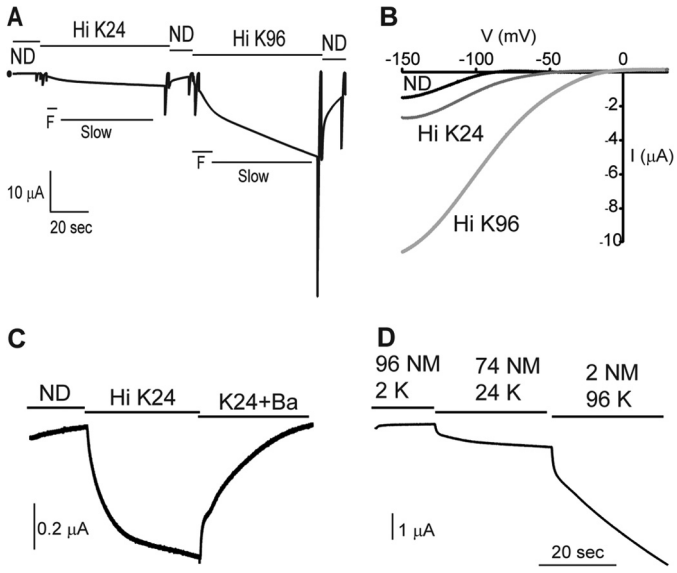

FIGURE 2. **Kir2.4 cloned from mouse retina shows its characteristic behavior.** *A*, sample current recorded from an oocyte that was injected with Kir2.4 (1 ng) and clamped to −80 mV. In this experiment, after ~10 s in ND96 (*ND*), the solution was changed to high K^+ 24 (*Hi K24*) for 1 min, then to ND96 briefly, then to high K^+ 96 (*Hi K96*) for 1 min, and finally to ND96. Ramps from −130 to +30 mV were applied at the ends of ND96 and at the beginnings and ends of high K^+ 24 and high K^+ 96 applications; they are seen as the fast downward trace followed by an upward deflection. Immediately after the solution is changed to high K, the inward current shows a fast increase (*F*) and then a slower increase (*slow*). When the solution is switched back to ND96, the base line does not return to its initial value quickly. *B*, ramp responses are shown in an expanded time scale for ND96, high K^+ 24, and high K^+ 96. *C*, when 5 mM barium replaces 5 mM Na^+ (*K24+Ba*), the current that is evoked by high K^+ 24 is completely blocked. *D*, replacing Na^+ with $NMDG^+$ (*NM*) does not affect the K^+-induced current. Time scale in *D* also applies to *C*.

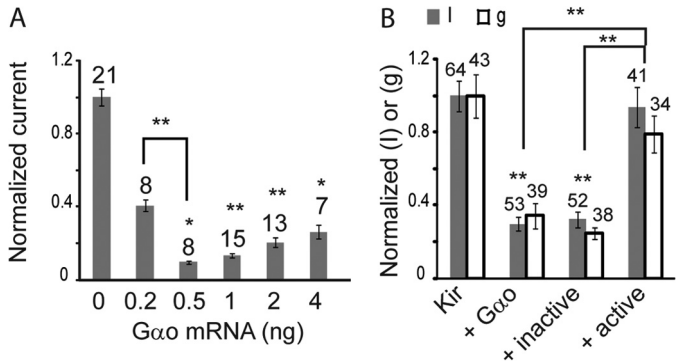

FIGURE 3. **Inactive but not constitutively active $G\alpha_o$ decreases basal Kir2.4 current.** *A*, average normalized currents for oocytes injected with Kir2.4 mRNA (1 ng) and the indicated amounts of $G\alpha_o$ mRNA. For current recordings, oocytes were clamped at −80 mV. For all bar graphs, *error bars* indicate S.E., and *numbers above bars* indicate number of oocytes recorded for each group. *, significant ($p < 0.05$) difference from the group injected with only Kir2.4; **, highly significant ($p < 0.01$) difference. Wild type $G\alpha_o$ at relatively low amounts decreases the basal current in a dose dependent manner because current with 0.5 ng was significantly different from 0.2 ng of $G\alpha_o$. Current with 2 or 4 ng was not significantly different from 0.5 or 1 ng. *B*, average normalized currents (*gray bars*) and slope conductances (*white bars*) for oocytes injected with Kir2.4 mRNA (1 ng) alone, or with Kir2.4 and 1 ng of the following: wild type, constitutively inactive (G204A), or constitutively active (Q205L) $G\alpha_o$. The reduction in basal current of oocytes co-injected with wild type or inactive $G\alpha_o$ are highly significant when compared with the current in oocytes co-injected with active $G\alpha_o$, indicated by *brackets*.

tion, and the holding current was measured before and after switching to 24 mM external K^+ concentration (henceforth called high K) or occasionally to 96 mM K^+ concentration (high K96). Upon switching the medium from ND96 to high K or to high K96, the oocyte showed an increase in inward current that was accompanied by an increase in slope conductance (Fig. 2, *A* and *B*). This increase in current occurred in two phases, a fast phase that probably depended on the perfusion rate, and a very slow phase that lasted more than 15 min (Fig. 2*A*). This two-phase response has been reported previously for human retinal Kir2.4 (22). Notably, although the current was dramatically reduced when the solution switched from high K back to ND96, a residual "memory" of the high K^+ effect remained as the current did not return to its initial low level even after 20 min. Consistent with earlier reports (21, 22), this K^+ current was blocked by barium: 2 mM reduced the current by 60% and 5 mM totally eliminated it (Fig. 2*C*). Although K^+-selective channels are usually not blocked by extracellular Na^+, the delayed rectifying potassium channel in bullfrog sympathetic neurons is an exception (27). Thus, we tested whether the slow increase in inward current after switching to high K^+ was due to release from Na^+ block by replacing Na^+ with the impermeant cation $NMDG^+$. We found that neither total substitution of Na^+ with $NMDG^+$ (Fig. 2*D*) nor switching from 24 mM $NMDG^+$ + 72 mM Na^+ solution to Hi K^+ solution (*i.e.* without changing Na^+ concentration; data not shown) affected this slow conductance increase, suggesting that the behavior is not due to Na^+ block.

Kir2.4 Basal Current Is Reduced by $G\alpha_{o1}$—We wondered whether Kir2.4 might be modulated by heterotrimeric G-proteins in a manner similar to Kir3. We therefore investigated the effect of $G\alpha_{o1}$ on the Kir2.4 basal current and inward conductance. Because the inward current under high K^+ did not plateau in a reasonable time, measurements of this basal current were taken one and/or 2 min after switching solutions. For conductance measurements, we ramped the oocytes from −150 mV to +30 mV and calculated the slope of the *I-V* curve in the linear range (Fig. 2*B*). When small amounts of $G\alpha_{o1}$ were co-expressed with Kir2.4, the basal current decreased dramatically in a dose-dependent manner (Fig. 3*A*, total of three experiments). Injection of 0.2 ng of $G\alpha_{o1}$ reduced the current to ~40% of the control level, and injection of 0.5 ng decreased it to ~10%. Higher amounts did not reduce the current further; current was insignificantly higher than that with 0.5 ng of $G\alpha_{o1}$ but still significantly lower than Kir2.4 alone. For the rest of our experiments, unless otherwise stated, we used 1 ng of $G\alpha_{o1}$. Co-injecting $G\alpha_{o1}$ also affected the zero-crossing potential, *i.e.* the potential at which no net current passes through the membrane and thus reflects the resting potential of the oocyte. Although uninjected oocytes showed an average potential of ~−15 mV, oocytes expressing Kir2.4 under ND96 showed −27 mV (due to a maintained outward K^+ current), and those expressing Kir2.4 + $G\alpha_{o1}$ showed a potential similar to uninjected oocytes of ~−15 mV, suggesting a reduced basal outward K^+ current. The reduction in current and conductance induced by the wild type form was also observed with a mutant form of $G\alpha_{o1}$ that renders this subunit constitutively inactive (G204A) but was not seen with the constitutively active form (Q205L) (Fig. 3*B*). As for this experiment and for all experiments henceforth, the observed effects remained the same regardless of whether we measured current at 1 or 2 min after the switch to high K, and

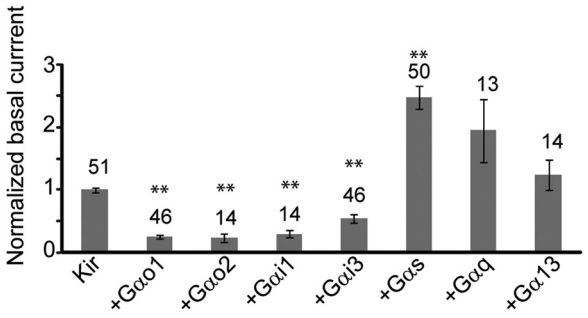

FIGURE 4. **$G\alpha_{o/i}$ reduces basal current, whereas $G\alpha_s$ increases it.** Normalized basal currents ($V = -80$ mV) for oocytes injected with Kir2.4 (1 ng) alone or with Kir2.4 and one of the indicated $G\alpha$ subunits (1 ng). *Error bars* are S.E., and significance is as described in the legend to Fig. 3.

regardless of whether we measured inward current or slope conductance. Therefore, the following figures show only the relative basal currents.

We next determined the specificity of $G\alpha$. We injected several species of $G\alpha$ subunits and found that all the $G\alpha_{i/o}$ tested, $G\alpha_{o2}$, $G\alpha_{i1}$, and $G\alpha_{i3}$, were as effective as $G\alpha_{o1}$ in reducing the Kir2.4 basal current, with the difference between these groups and the group injected with only Kir2.4 being highly significant (Fig. 4). In contrast, $G\alpha_s$ dramatically increased the Kir current (by 2.4-fold; $p \ll 0.01$). $G\alpha_q$ also increased the current, but to a lesser extent than $G\alpha_s$ (1.5-fold) and without significance, whereas $G\alpha_{13}$ did not change it. In the remaining experiments, we used only $G\alpha_{o1}$ (and refer to it as $G\alpha_o$)

Kir2.4 Basal Current Is Increased by Gβγ—Following the model of Kir3, we hypothesized that the reduction of Kir2.4 current by co-expressing $G\alpha_{o/i}$ is due to scavenging $G\beta\gamma$ that might be required to gate the channel. Thus, we tested the effect of co-expressing $G\beta1\gamma2$ and found that it increased the basal current in a dose-dependent manner (Fig. 5*A*). Injecting 1 ng of $G\beta1$ + 0.2 ng of $G\gamma2$ increased the current by ~2-fold (five experiments). Doubling the amount of each subunit increased the current 5-fold (three experiments), and tripling it increased the current almost 9-fold (one experiment). Moreover, $G\beta\gamma$ counteracted the effect of $G\alpha_o$ when these subunits were co-injected, and this effect was dose-dependent as well. Injecting 5 ng of $G\beta$ +1 ng of $G\gamma$ in addition to 1 ng of $G\alpha_o$ increased the current more than 2-fold relative to that of Kir2.4 alone, and more than 8-fold relative to that of Kir + 1 ng $G\alpha_o$ (Fig. 5*B*, compare *second bar* to *rightmost bar*). When we compare the ratio of oocytes injected with Kir2.4+$G\beta\gamma$ to Kir2.4 alone, and that of Kir2.4+$G\alpha_o$+$G\beta\gamma$ to that of Kir2.4+$G\alpha_o$, it appears that higher expression of $G\beta\gamma$ are needed to lift the base line when $G\alpha_o$ is co-expressed because the potency of $G\alpha_o$ is greater than $G\beta\gamma$. Although 1 ng of $G\alpha_o$ decreases the current by ~5-fold relative to Kir alone, 1 ng of $G\beta$ + 0.2 ng of $G\gamma$ increase the current by only ~2-fold. To determine whether the effect of $G\beta\gamma$ is specific and whether endogenous $G\beta\gamma$ would have a similar effect to exogenously added subunits, we injected phosducin, a molecule that is known to scavenge $G\beta\gamma$ without affecting GTP binding to $G\alpha$. This reduced the current to ~50% (with 1 ng of phosducin) or ~20% (with 2 and 4 ng). The effect of phsoducin could be reversed by adding $G\beta\gamma$ (Fig. 5*C*, altogether four experiments). Our findings suggest that $G\beta\gamma$ modulates Kir2.4 activity and pertussis toxin-sensitive $G\alpha$ acts to scavenge $G\beta\gamma$. This interpretation is consistent with inactive $G\alpha$ being more effective than active $G\alpha$ because the inactive form has a much higher affinity for $G\beta\gamma$. However, it may be inconsistent with the finding that $G\alpha_s$ increases basal expression.

Kir2.4 Surface Expression Is Reduced by $G\alpha_o$—If $G\beta\gamma$ gates the Kir2.4 channel as it gates Kir3, it should be possible to activate the channels by co-expressing a G-protein-coupled receptor. Thus, we co-expressed the muscarinic receptor M2, $G\alpha_o$, and the Kir2.4 or Kir3.1/2 channels. When the receptor and $G\alpha_o$ were expressed with Kir3.1/2, application of 20 micromolar acetylcholine activated the channel. However, when they were co-expressed with Kir2.4, no such activation could be observed (data not shown). Similar experiments using the metabotropic glutamate receptor mGluR6 instead of the muscarinic receptor showed that glutamate evoked Kir3.1/2 current (see Ref. 2) but not Kir2.4 current. Thus, we suspected that the observed G-protein modulation of the Kir2.4 channel results indirectly by affecting trafficking or expression. We tested this hypothesis by expressing Kir2.4 fused to cerulean (Kir-cer).

We first performed some control experiments. We confirmed that Kir-cer has the same channel properties as the wild type Kir2.4 (data not shown). We also determined that our measurements of surface fluorescence were meaningful. To this end, we expressed different amounts of Kir-cer mRNA and recorded the surface fluorescence to verify that the fluorescence is linearly related to the injected amount (Fig. 6, *A* and *B*). Next, we injected oocytes with 5 or 10 ng of Kir-cer and used nine oocytes from each group to measure both the basal current and the surface fluorescence. We found that the current correlated well with the fluorescence (Fig. 6*C*), confirming the validity of the method for measuring surface expression.

To determine the effect of G-protein subunits on surface expression of the Kir2.4 channel, we measured the inward current and surface fluorescence for groups of oocytes that were co-injected with mRNA for $G\alpha_{o1}$ and $G\beta\gamma$. Injection of 1 ng of Kir2.4-cer yielded very low fluorescent measurements that were similar to the measured autofluorescence. We therefore had to inject greater amounts (but not too great to keep the current within a reasonable range of less than 2 μA for Kir2.4 alone); we therefore settled on 4 ng of Kir2.4-cer mRNA. We found that 0.5 ng of $G\alpha_o$ mRNA reduced the basal current down to 23% of Kir alone, and the surface fluorescence to 13% (Fig. 6, *D* and *E*). One ng of $G\alpha_o$ mRNA further reduced the current to 4% and the fluorescent to noise level. Adding $G\beta\gamma$ mRNA to 0.5 ng of $G\alpha_o$ mRNA increased both fluorescent intensity (by 4-fold) and basal current (by 2-fold). The relative increase in current and fluorescence was not identical due to limitations in determining surface expression when expression is low and gets close to autofluorescence level shown by uninjected oocytes. Nevertheless, the basal current correlated pretty well with the measured surface expression ($R^2 = 0.92$; Fig. 6*F*). We therefore suggest that all the effects that we have observed with the basal current could be explained by the G-protein subunits having affected the expression or the trafficking of Kir2.4.

Differential Distribution of Kir2.4 in Transfected HEK Cells—To test whether G-protein subunits affect Kir2.4 localization in

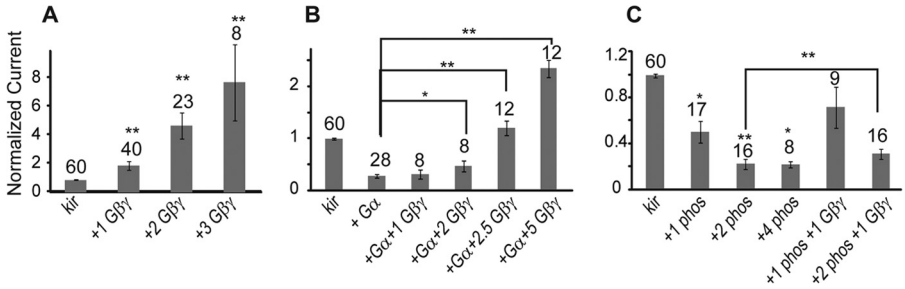

FIGURE 5. **Gβγ increases the basal current of Kir2.4 when injected either alone or with proteins that sequester it.** *A*, normalized basal currents for oocytes injected with mRNA for Kir2.4 (1 ng) alone or Kir2.4 + indicated amount (in ng) for Gβ1 + one-fifth of this amount for Gγ2; ($V = -80$ mV). A *t* test was performed against Kir2.4 alone. *Error bars* are S.E., and significance is as described in the legend to Fig. 3. *B*, normalized basal currents for oocytes injected with Kir2.4 (1 ng) alone, Kir2.4 + $G\alpha_o$ (1 ng), or Kir2.4 + $G\alpha_o$ + indicated amount for Gβ1 + 1/5 of this amount for Gγ2. A *t* test compares currents between oocytes with Kir2.4 + $G\alpha_o$ to those with additional Gβγ (indicated by *brackets*). *C*, normalized basal currents for oocytes injected with Kir2.4 (1 ng) alone, Kir2.4 + additional phosducin (*phos*) as indicated (in ng), or Kir2.4 + phosducin + Gβγ as indicated. When *no bracket* is shown, *t* test compares that particular group to the Kir2.4 group.

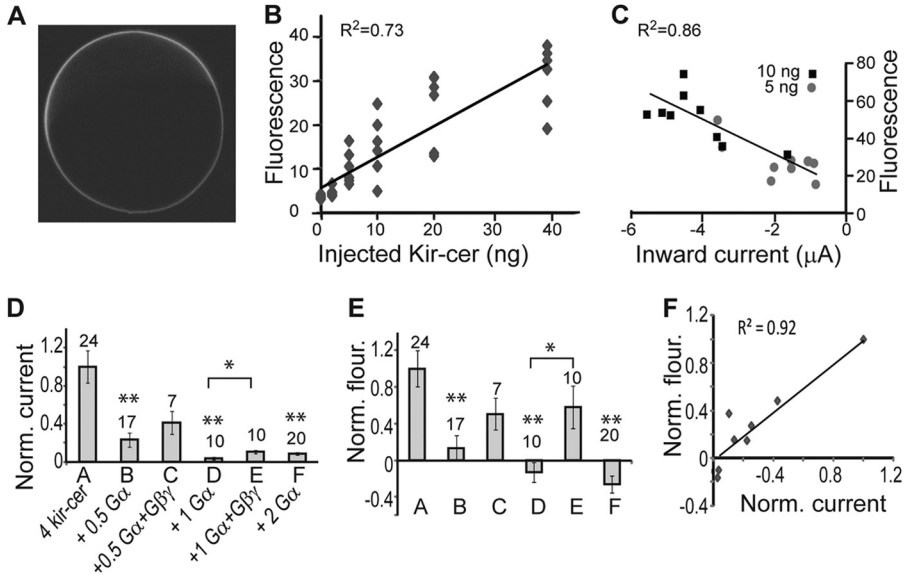

FIGURE 6. **Heterotrimeric G-protein subunits affect Kir2.4 surface expression.** *A*, confocal image of an oocyte injected with 5 ng of Kir-cer and imaged 3 days later under a 10× water immersion objective. *B*, the measured surface fluorescence is linearly related to the amount of injected Kir2.4 mRNA. R^2 is the correlation coefficient for these data. *C*, the measured surface fluorescence correlates well with the inward current. Data points are for 5 and 10 ng of injected Kir2.4 from a different experiment than in *B*. *D*, normalized (*Norm.*) basal currents for oocytes injected with various mRNAs for kir-cer (4 ng) alone (condition A, 4 kir-cer), and 4 ng kir-cer + various amounts of G-protein subunits (condition B, 0.5 ng of $G\alpha_o$; condition C, 0.5 ng of $G\alpha_o$ + 10 ng of Gβ1 + 2 ng of Gγ2; condition D, 1 ng of $G\alpha_o$; condition E, 1 ng of $G\alpha_o$ + 5 ng of Gβ1 + 1 ng of Gγ2; or condition F, 2 ng of $G\alpha_{o1}$). *E*, normalized surface fluorescence (*Norm. fluor.*) for the same oocyte groups as in *D*. Oocytes with high amounts of Gα display negative values because the autofluorescence of uninjected oocytes is relatively high and variable, and here it happened to be higher than the fluorescence of these groups. Unless otherwise indicated by *brackets*, *asterisks* indicate the significant difference compared with results for Kir-cer injection alone; a *single asterisk* indicates $p < 0.05$ and *double asterisks* indicate $p < 0.01$. *F*, normalized fluorescence measurements for each group in each experiment is plotted against the normalized basal current showing that these are correlated ($R^2 = 0.92$); data are taken from the experiments in *D* and *E*; n = three experiments (conditions B and F were repeated twice).

mammalian cells, we transfected HEK293 cells with Kir-cer alone, Kir-cer + $G\alpha_{o1}$, or Kir-cer + Gβ1γ2 (Fig. 7). To identify cells that were cotransfected, slides were immunostained for $G\alpha_o$ or Gβ1. Expression of Kir-cer varied in different cells; in few cells, a clear outline of the cells could be seen, suggestive of membrane localization; in some, the expression was restricted to the intracellular milieu, where it concentrated near the nucleus (presumably on the Golgi apparatus; as in Fig. 7*E*); and in others, Kir-cer appeared in both of these locations (as in Fig. 7, *A–D*). Interestingly, when Kir2.4 was co-expressed with Gβγ, these proteins perfectly colocalized within intracellular microdomains and on the plasma membrane (Fig. 7, *B–D*). We counted the number of cells in which a clear outline appeared and those in which Kir-cer was restricted to the cytosol and computed the percentage of those with membrane localization to the total number. In cells expressing only Kir-cer, the percentage was 67% (63 cells); in cells expressing Kir-cer+$G\alpha_{o1}$ (Fig. 7*E*), it was 39% (44 cells); and in those expressing Kir2-cer+Gβ1γ2 (Fig. 7*D*), it was 78% (n = 37). To further assess these results by a different method, we drew lines across cells and plotted the intensities along these lines (Fig. 7, *F* and *G*). This representation provides a semiquantitative visual display of the relative distribution of Kir2.4 near or at the membrane (on the *left* of the graph) to that in the cytosol (broad staining on the *right*). In all cases, cytosolic expression was much stronger than membranal staining. However, when Kir2.4 co-expressed with Gβγ, in most cells staining intensity was sharp near the membrane (Fig. 7, *H* and *I*). When Kir2.4 was co-expressed with $G\alpha_{o1}$, membranal staining was weaker (Fig. 7*E*, *J* and *K*). Thus, we conclude that as in oocytes, $G\alpha_o$ overexpressed in HEK cells

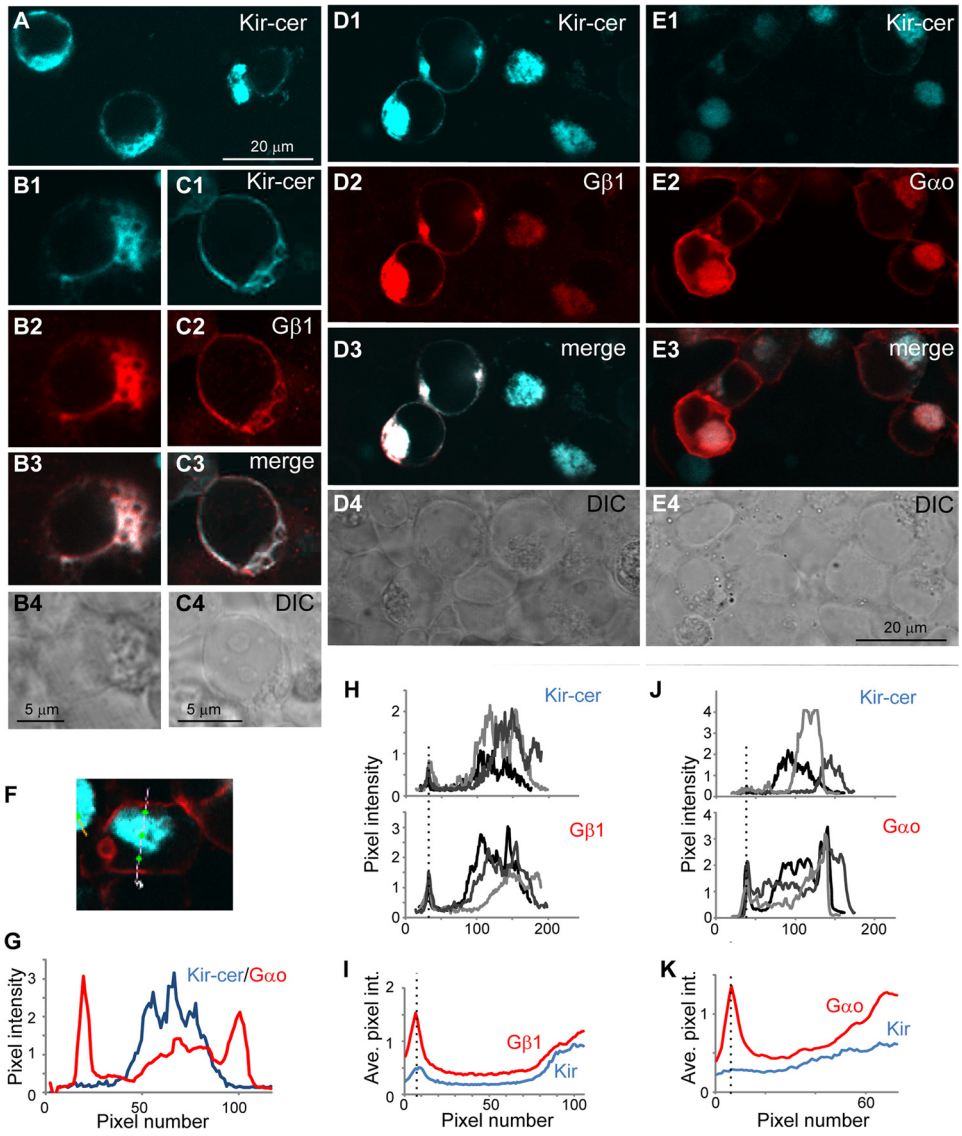

FIGURE 7. **G-proteins affect intracellular distribution of Kir2.4.** *A–F*, confocal images of transfected HEK cells. *A*, cells were transfected with Kir2.4-cer alone and visualized by their fluorescent signal; *B–D* and *F*, cells were transfected with Kir2.4-cer + Gβ1 +Gγ2 and visualized as indicated; *E*, cells were transfected with Kir2.4-cer + $G\alpha_{o1}$ and visualized as indicated. Note in *B* and *C* the exquisite colocalization of Kir2.4 (*cyan*) and Gβ1 (*red*). *F*, an example of cell transfected with Kir2.4-cer + $G\alpha_{o1}$ with a *line drawn through it*; the *line* begins at the lower point. *G*, intensity profiles for Kir2.4 and $G\alpha_o$ along the line in *F*. In this cell, no Kir2.4 expression at or near the membrane could be detected. *H*, examples of intensity profiles for Kir-cer (*top*) and Gβ1(*bottom*) for three cells (drawn in three *gray shades*) co-transfected with Kir-cer + Gβ1 + Gγ2. *I*, average (*Ave.*) intensity profiles for 32 cells transfected and viewed as described above. *J*, three examples of intensity (*int.*) profiles for Kir-cer (*top*) and $G\alpha_o$ (*bottom*) for cells co-transfected with plasmids encoding these proteins. *K*, average intensity profiles for 36 cells transfected and viewed as indicated. *Dotted lines* show membrane locations as determined by staining for $G\alpha_o$ or Gβ1. The *scale bar* in *E4* applies to all *D* and *E panels*.

appeared to reduce surface expression, whereas Gβγ increases it. Unlike in oocytes where it was possible to image Kir-cer surface expression without contribution from cytosolic expression, imaging HEK cells does not provide the required resolution to discriminate these because cytosolic expression near the membrane will be lumped with that of the membrane. Thus, it is possible that the effect in HEK cells is larger than seen. It should also be noted that HEK cells express Gβ1 endogenously, perhaps contributing to Kir2.4 surface expression when transfected alone.

Kir2.4 in the Dendritic Tips of Retinal ON Bipolar Cells Is Reduced in the Absence of Gβ3—To see whether our findings in oocytes are also relevant to neural tissue, we immunostained wild type retina and *Gnb3* (gene encoding Gβ3)-null retina for Kir2.4. We have previously shown that Kir2.4 is expressed in the dendritic tips of ON bipolar cells (5). The antibody against Kir2.4 revealed punctate staining that often showed two populations of puncta, a brightly stained population that we judge to be noise and a faintly stained population that colocalized well with the staining for mGluR6, the G-protein-coupled receptor that mediates the light response in these cells (Fig, 8, *left column*). In *Gnb3*-null retinas (four sets of experiments), the puncta that stained for Kir2.4 and colocalized with mGluR6 were greatly reduced in their intensity. Staining of bipolar cell somas in the inner nuclear layer was also slightly reduced in the null retina but to a lesser extent than the dendritic tips. As shown previously, staining for mGluR6 was also slightly reduced (Fig. 8, *right column*) (26). Unlike *Gnb3*-null retina,

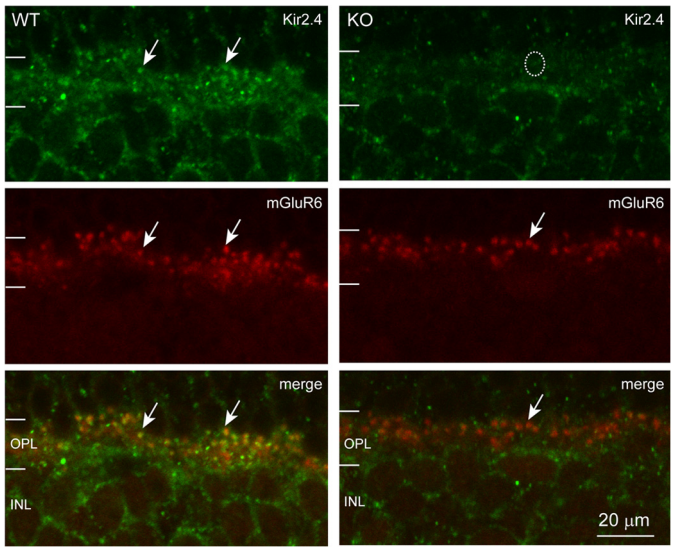

FIGURE 8. **Gβ3 deletion affects Kir2.4 localization in retinal ON bipolar cells.** Double immunostaining of radial retinal sections for Kir2.4 (*green*) and mGluR6 (*red*) in wild type (*left column*) and *Gnb3*-null (*right column*) retinas. *OPL*, outer plexiform layer; *INL*, inner nuclear layer. With either Kir2.4 or mGluR6 staining, puncta intensity (*arrows*) is reduced in the null retina; the *dotted circle* on the KO image represents an unstained dendritic tip. Somas in the inner nuclear layer mainly represent ON bipolar cells, and their staining was also slightly reduced.

staining of *Gnao1* (gene encoding $G\alpha_{o1}$)-null retina was not much different from the wild type (data not shown).

DISCUSSION

We show here that different types of G-protein subunits affect the basal current and surface expression of Kir2.4. Although $G\alpha_{o/i}$ reduces this current, $G\alpha_s$ and $G\beta\gamma$ increase it. We also show that the effects on basal current are correlated with the effects on surface expression, and we suggest that the former results from the latter. We further show that, when co-expressed, $G\alpha_o$ and Kir2.4 interact in retina and in HEK cells. Given that $G\alpha$ and $G\beta\gamma$ affect expression in an opposing manner, it would be informative to know which of these subunits mediates the surface expression. On the one hand, it may be that free $G\beta\gamma$ helps traffic the channel to the plasma membrane. On the other hand, it is possible that $G\alpha_o$-GDP binds Kir2.4 and prevents it from moving to the plasma membrane or sends it for degradation, as may be suggested by preliminary results showing that not only surface expression but also total expression of Kir2.4 is reduced by co-injecting $G\alpha_o$.

Gβγ as a Player in Trafficking—Our measurements of currents and fluorescence can most easily be explained assuming that mediation by the $G\beta\gamma$ dimer; *i.e.* free $G\beta\gamma$ helps transport the channel to the plasma membrane. Thus, co-expression of $G\beta\gamma$ with Kir2.4 increases channel expression because $G\beta\gamma$ is overexpressed and a good fraction of these subunits remain as free $G\beta\gamma$. Adding $G\alpha_o$ reduces channel expression because $G\alpha_o$ sequesters endogenous free $G\beta\gamma$ and leaves a smaller fraction of these dimers available for trafficking. Co-expressing $G\beta\gamma$ and $G\alpha$ yields intermediate currents whose magnitude depends on the ratio of the expressed subunits. Most significantly, phosducin, which binds $G\beta\gamma$ without affecting the activity state of $G\alpha$, reduces the current, and this effect is reversed by co-expressing $G\beta\gamma$. Our interpretation is also consistent with the finding that $G\alpha_oGA$ (inactive), and not $G\alpha_oQL$ (active), reduces the current because only $G\alpha_oGA$ significantly binds $G\beta\gamma$ and sequesters it. If we assume the alternative explanation that only $G\alpha_o$-GDP mediates the observed effects, it would be difficult to explain how overexpression of $G\beta\gamma$ increases Kir2.4 expression (unless we assume that a fraction of endogenous $G\alpha$-GDP exists as a monomer and is being sequestered by $G\beta\gamma$), how phosducin reduces the current, and how $G\beta\gamma$ reverses the effect of phosducin. One puzzling question is why $G\alpha_s$ does not decrease basal current because it should be able to bind $G\beta\gamma$ just as well as $G\alpha_{o/i}$. This may be explained by additional factors that affect surface expression such as cAMP, whose concentration can be increased by overexpression of $G\alpha_s$ (*e.g.* Ref. 28).

The effect of G-proteins on trafficking has been studied in several systems. Co-expressing Kir3.2 with $G\alpha_{i3}$ or $G\beta\gamma$ in oocytes affects Kir3.2 surface expression in a similar way as it affects Kir2.4 (16). The function of $G\beta\gamma$ in controlling trafficking was also studied (reviewed by Refs. 29 and 30). The mechanism of its action is attributed mostly to the direct stimulation of protein kinase D located in the Golgi apparatus (31–33). In a more recent study where the effect of $G\beta\gamma$ on transport was investigated, $G\beta\gamma$ was shown to localize to the Golgi in HeLa cells and to facilitate transport of cargo to the plasma membrane. This transport was inhibited by gallein, a small molecule inhibitor of $G\beta\gamma$, and by a $G\beta\gamma$ scavenger (GRK2ct) that was directed to the Golgi (34). A role for $G\beta\gamma$ in trafficking is also supported by studies in neural tissue. We have recently shown that in retinal ON bipolar cells lacking Gβ3 (a subunit that mediates their light responses by coupling the metabotropic mGluR6 receptor to the TRPM1 channel), numerous elements that play an important role in the mGluR6 cascade are down-regulated or redistributed (26). This includes not only the G-protein subunit partners, but also the receptor mGluR6 and the channel TRPM1. The most dramatic effect was seen on the expression of the GTPase activating complex (comprised of Gβ5, RGS7/11, and R9AP). In wild type, this complex was highly localized to the dendritic tips of the ON bipolar cells, but in Gβ3-null cells, all of the elements of this complex were hardly detectable. In this study, we added Kir2.4 to the list of proteins whose localization is affected by deletion of Gβ3. Some of these effects on localization may be indirect, resulting from a lack of activity. However, some are probably direct because we see a greater effect in cells lacking Gβ3 than those lacking $G\alpha_{o1}$, another subunit required for the light response of this cell (3 and this work) (40).

Possible Role of $G\alpha_o$—Although all of our data can be qualitatively explained by assuming that $G\beta\gamma$ alone traffics Kir2.4, it is still possible that $G\alpha_{o/i}$ contributes directly to the stability of Kir2.4, to its trafficking to the plasma membrane, or to regulation of its basal current. The role of $G\alpha$ in stability has been shown in Neuro-2A cells where $G\alpha_{o/i2}$-GDP directed Rap1GAPII for proteasomal degradation (thereby activating Rap1 and inducing neurite outgrowth) (35). The function of $G\alpha$ in trafficking has been shown in LLC-PK1 cells, where overexpression of $G\alpha_{i3}$ tonically represses trafficking of heparin sulfate proteoglycan through the Golgi apparatus (36). The direct effect of $G\alpha_{i3}$ on Kir current (which is independent of its role as

a G$\beta\gamma$ donor) has been shown in *Xenopus* oocytes where it binds GIRK1, reduces the basal current of Kir3.1/2 channels and simultaneously improves the activation of the channel by G$\beta\gamma$ (15, 16). Interestingly, Gα_{i3} does not bind Kir3.2, so it does not affect the basal current of homomeric Kir3.2.

In light of these diverse possible roles for Gα subunits, it is possible that G$\alpha_{o/i}$ in oocytes also affects the basal current of Kir2.4 independently of its effect through G$\beta\gamma$. Some support for this notion comes from the interaction we observe between Gα_{o1} and Kir2.4 in retina and in HEK cells transfected with these genes. Similar to Kir3.1, whose current is affected primarily by the GDP-bound form of Gα, interaction of Gα_o with Kir2.4 is stronger in the Gα-GDP conformation (as indicated by stronger interaction in the absence of AlF_4^-), and this is consistent with the current being reduced by Gα_{o1}GA but not Gα_{o1}QL. In addition, although the interaction we observe using co-immunoprecipitation could have occurred through G$\beta\gamma$, the interaction we initially saw in yeast should have been direct.

Possible Implication of Kir2.4 Regulation in Neurons—The properties of the Kir2.4 channels have mostly been studied in expression systems where the channel is probably a homomer, but Kir2.4 has been shown to form a functional channel with Kir2.1 (24). Although the Kir2.4 homomer (or monomer) largely accumulates at the Golgi apparatus with only a small fraction being targeted to the plasma membrane, a large fraction of Kir2.1 is targeted to the plasma membrane. The targeting signal in the Kir2.1 sequence has been identified and has been shown to target also the Kir2.4-Kir2.1 heteromer to the plasma membrane (37). In retina, many cell types including horizontal cells and certain types of bipolar cells are found to exhibit Kir current (38, 39). Correspondingly, immunostaining for Kir2.4 is abundant in retina, and ON bipolar cells display a punctate pattern with high concentrations at their somas and their dendritic tips where they receive input from photoreceptors (Ref. 5 and this work). If Kir2.4 does oligomerize with another Kir2 member in ON bipolar cells, its trafficking is likely controlled by the nature of the oligomer with additional regulation by the G-proteins in these cells. Given that Kir2.4 is strongly inwardly rectifying, it will contribute little to the membrane potential at rest or during depolarization because its outward conductance is probably too small. However, when neurons are depolarized for a long time, the extracellular K^+ concentration increases. Then the Kir channel can prevent excessive K^+ accumulation with its inward current and can help recover the resting membrane potential. Thus, targeting Kir to the active regions within a cell via G-proteins may represent an efficient mechanism because the activity of many neurons is already mediated by G-proteins.

Acknowledgments—We thank Dr. Nathan Dascal for numerous discussions and suggestions during the initial phase of this work and for generously contributing numerous clones and reagents. We thank Dr. David Manning for the Gα_{o1} clone and the rabbit anti-Gα_o, Dr. Lutz Birnbaumer for the Gα_{o2} clone and the Gnao1-null mouse, Dr. Kirill Martemyanov for Gβ1 and Gγ2 clones, Dr. Rudiger Veh for the anti-Kir2.4, and Dr. Rukki Rao-Mirotznik for editing.

REFERENCES

1. Wettschureck, N., and Offermanns, S. (2005) Mammalian G proteins and their cell type specific functions. *Physiol. Rev.* **85,** 1159–1204
2. Dhingra, A., Faurobert, E., Dascal, N., Sterling, P., and Vardi, N. (2004) A retinal-specific regulator of G-protein signaling interacts with Gα_o and accelerates an expressed metabotropic glutamate receptor 6 cascade. *J. Neurosci.* **24,** 5684–5693
3. Dhingra, A., Jiang, M., Wang, T. L., Lyubarsky, A., Savchenko, A., Bar-Yehuda, T., Sterling, P., Birnbaumer, L., and Vardi, N. (2002) Light response of retinal ON bipolar cells requires a specific splice variant of Gα_o. *J. Neurosci.* **22,** 4878–4884
4. Dhingra, A., Lyubarsky, A., Jiang, M., Pugh, E. N., Jr., Birnbaumer, L., Sterling, P., and Vardi, N. (2000) The light response of ON bipolar neurons requires Gαo. *J. Neurosci.* **20,** 9053–9058
5. Dhingra, A., Sulaiman, P., Xu, Y., Fina, M. E., Veh, R. W., and Vardi, N. (2008) Probing neurochemical structure and function of retinal ON bipolar cells with a transgenic mouse. *J. Comp. Neurol.* **510,** 484–496
6. Doupnik, C. A., Davidson, N., and Lester, H. A. (1995) The inward rectifier potassium channel family. *Curr. Opin. Neurobiol.* **5,** 268–277
7. Isomoto, S., Kondo, C., and Kurachi, Y. (1997) Inwardly rectifying potassium channels: their molecular heterogeneity and function. *Jpn J. Physiol.* **47,** 11–39
8. Wickman, K. D., Iñiguez-Lluhl, J. A., Davenport, P. A., Taussig, R., Krapivinsky, G. B., Linder, M. E., Gilman, A. G., and Clapham, D. E. (1994) Recombinant G-protein $\beta\gamma$-subunits activate the muscarinic-gated atrial potassium channel. *Nature* **368,** 255–257
9. Logothetis, D. E., Kurachi, Y., Galper, J., Neer, E. J., and Clapham, D. E. (1987) The $\beta\gamma$ subunits of GTP-binding proteins activate the muscarinic K^+ channel in heart. *Nature* **325,** 321–326
10. Dascal, N. (2001) Ion-channel regulation by G proteins. *Trends Endocrinol. Metab.* **12,** 391–398
11. Huang, C. L., Slesinger, P. A., Casey, P. J., Jan, Y. N., and Jan, L. Y. (1995) Evidence that direct binding of G $\beta\gamma$ to the GIRK1 G protein-gated inwardly rectifying K+ channel is important for channel activation. *Neuron* **15,** 1133–1143
12. Bichet, D., Haass, F. A., and Jan, L. Y. (2003) Merging functional studies with structures of inward-rectifier K(+) channels. *Nat. Rev. Neurosci.* **4,** 957–967
13. Rubinstein, M., Peleg, S., Berlin, S., Brass, D., and Dascal, N. (2007) Gα3 primes the G protein-activated K+ channels for activation by coexpressed G$\beta\gamma$ in intact *Xenopus* oocytes. *J. Physiol.* **581,** 17–32
14. Ivanina, T., Varon, D., Peleg, S., Rishal, I., Porozov, Y., Dessauer, C. W., Keren-Raifman, T., and Dascal, N. (2004) G i1 and Gi3 differentially interact with, and regulate, the G protein-activated K+ channel. *J. Biol. Chem.* **279**, 17260–17268.
15. Peleg, S., Varon, D., Ivanina, T., Dessauer, C. W., and Dascal, N. (2002). Gα (i) controls the gating of the G protein-activated K(+) channel, GIRK. *Neuron* **33**, 87–99
16. Rubinstein, M., Peleg, S., Berlin, S., Brass, D., Keren-Raifman, T., Dessauer, C. W., Ivanina, T., and Dascal, N. (2009) Divergent regulation of GIRK1 and GIRK2 subunits of the neuronal G protein gated K+ channel by GαiGDP and G$\beta\gamma$. *J. Physiol.* **587,** 3473–3491
17. Wang, J., Huang, Y., and Ning, Q. (2011) Review on regulation of inwardly rectifying potassium channels. *Crit. Rev. Eukaryot. Gene Expr.* **21,** 303–311
18. Yi, B. A., Minor, D. L., Jr., Lin, Y. F., Jan, Y. N., and Jan, L. Y. (2001) Controlling potassium channel activities: Interplay between the membrane and intracellular factors. *Proc. Natl. Acad. Sci. U.S.A.* **98,** 11016–11023
19. Shen, W., Tian, X., Day, M., Ulrich, S., Tkatch, T., Nathanson, N. M., and Surmeier, D. J. (2007) Cholinergic modulation of Kir2 channels selectively elevates dendritic excitability in striatopallidal neurons. *Nat. Neurosci.* **10,** 1458–1466
20. de Boer, T. P., Houtman, M. J., Compier, M., and van der Heyden, M. A. (2010) The mammalian K(IR)2.x inward rectifier ion channel family: expression pattern and pathophysiology. *Acta Physiol.* **199,** 243–256
21. Töpert, C., Döring, F., Wischmeyer, E., Karschin, C., Brockhaus, J., Bal-

lanyi, K., Derst, C., and Karschin, A. (1998) Kir2.4: a novel K+ inward rectifier channel associated with motoneurons of cranial nerve nuclei. *J. Neurosci.* **18,** 4096–4105
22. Hughes, B. A., Kumar, G., Yuan, Y., Swaminathan, A., Yan, D., Sharma, A., Plumley, L., Yang-Feng, T. L., and Swaroop, A. (2000) Cloning and functional expression of human retinal kir2.4, a pH-sensitive inwardly rectifying K(+) channel. *Am. J. Physiol. Cell Physiol.* **279,** C771–784
23. Prüss, H., Derst, C., Lommel, R., and Veh, R. W. (2005) Differential distribution of individual subunits of strongly inwardly rectifying potassium channels (Kir2 family) in rat brain. *Brain Res. Mol. Brain Res.* **139,** 63–79
24. Schram, G., Melnyk, P., Pourrier, M., Wang, Z., and Nattel, S. (2002) Kir2.4 and Kir2.1 K(+) channel subunits co-assemble: a potential new contributor to inward rectifier current heterogeneity. *J. Physiol.* **544,** 337–349
25. Dascal, N., Lotan, I., Longstaff, A., and Revest, P. (1992) Expression of exogenous ion channels and neurotransmitter receptors in RNA injected *Xenopus* oocytes in *Methods in Molecular Biology*, pp. 205–225, The Humana Press, Totowa, NJ
26. Dhingra, A., Ramakrishnan, H., Neinstein, A., Fina, M. E., Xu, Y., Li, J., Chung, D. C., Lyubarsky, A., and Vardi, N. (2012) Gbeta3 is required for normal light on responses and synaptic maintenance. *J. Neurosci.* **32,** 11343–11355
27. Block, B. M., and Jones, S. W. (1996) Ion permeation and block of M-type and delayed rectifier potassium channels. Whole-cell recordings from bullfrog sympathetic neurons. *J. Gen. Physiol.* **107,** 473–488
28. Holzapfel, H. P., Bergner, B., Wonerow, P., and Paschke, R. (2002) Expression of Gα(s) proteins and TSH receptor signalling in hyperfunctioning thyroid nodules with TSH receptor mutations. *Eur. J. Endocrinol.* **147,** 109–116
29. Bomsel, M., and Mostov, K. (1992) Role of heterotrimeric G proteins in membrane traffic. *Mol. Biol. Cell* **3,** 1317–1328
30. Dupré, D. J., Robitaille, M., Rebois, R. V., and Hébert, T. E. (2009) The role of Gβγ subunits in the organization, assembly, and function of GPCR signaling complexes. *Annu. Rev. Pharmacol. Toxicol.* **49,** 31–56
31. Bard, F., and Malhotra, V. (2006) The formation of TGN-to-plasma-membrane transport carriers. *Annu. Rev. Cell Dev. Biol.* **22,** 439–455
32. Jamora, C., Yamanouye, N., Van Lint, J., Laudenslager, J., Vandenheede, J. R., Faulkner, D. J., and Malhotra, V. (1999) Gβγ-mediated regulation of Golgi organization is through the direct activation of protein kinase D. *Cell* **98,** 59–68
33. Jamora, C., Takizawa, P. A., Zaarour, R. F., Denesvre, C., Faulkner, D. J., and Malhotra, V. (1997) Regulation of Golgi structure through heterotrimeric G proteins. *Cell* **91,** 617–626
34. Irannejad, R., and Wedegaertner, P. B. (2010) Regulation of constitutive cargo transport from the trans-Golgi network to plasma membrane by Golgi-localized G protein βγ subunits. *J. Biol. Chem.* **285,** 32393–32404
35. Jordan, J. D., He, J. C., Eungdamrong, N. J., Gomes, I., Ali, W., Nguyen, T., Bivona, T. G., Philips, M. R., Devi, L. A., and Iyengar, R. (2005) Cannabinoid receptor-induced neurite outgrowth is mediated by Rap1 activation through G(α)o/i-triggered proteasomal degradation of Rap1GAPII. *J. Biol. Chem.* **280,** 11413–11421
36. Stow, J. L., de Almeida, J. B., Narula, N., Holtzman, E. J., Ercolani, L., and Ausiello, D. A. (1991) A heterotrimeric G protein, Gαi-3, on Golgi membranes regulates the secretion of a heparan sulfate proteoglycan in LLC-PK1 epithelial cells. *J. Cell Biol.* **114,** 1113–1124
37. Hofherr, A., Fakler, B., and Klöcker, N. (2005) Selective Golgi export of Kir2.1 controls the stoichiometry of functional Kir2.x channel heteromers. *J. Cell Sci.* **118,** 1935–1943
38. Perlman, I., Knapp, A. G., and Dowling, J. E. (1988). Local superfusion modifies the inward rectifying potassium conductance of isolated retinal horizontal cells. *J. Neurophysiol.* **60**, 1322–1332
39. Ma, Y. P., Cui, J., Hu, H. J., and Pan, Z. H. (2003) Mammalian retinal bipolar cells express inwardly rectifying K+ currents (IKir) with a different distribution than that of Ih. *J. Neurophysiol.* **90,** 3479–3489
40. Tummala, S., Fina, M., Dhingra, A., and Vardi, N. (2012) ARVO Abstract 4314/A540